

Topological Dimensions from Disorder and Quantum Mechanics?

Ivan Horváth^{1,2,*} and Peter Markoš^{3,†}

¹*Nuclear Physics Institute CAS, 25068 Řež (Prague), Czech Republic*

²*University of Kentucky, Lexington, KY 40506, USA*

³*Dept. of Experimental Physics, Faculty of Mathematics, Physics and Informatics, Comenius University in Bratislava, Mlynská Dolina 2, 842 28 Bratislava, Slovakia*

(Dated: Dec 18, 2022)

We have recently shown that critical Anderson electron in $D=3$ dimensions effectively occupies a spatial region of infrared (IR) scaling dimension $d_{\text{IR}} \approx 8/3$. Here we inquire about the dimensional substructure involved. We partition space into regions of equal quantum occurrence probability, such that points comprising a region are of similar relevance, and calculate the IR scaling dimension d of each. This allows us to infer the probability density $p(d)$ for dimension d to be accessed by electron. We find that $p(d)$ has a strong peak at d very close to 2. In fact, our data suggests that $p(d)$ is non-zero on the interval $[d_{\text{min}}, d_{\text{max}}] \approx [4/3, 8/3]$ and may develop a discrete part (δ -function) at $d=2$ in infinite-volume limit. The latter invokes the possibility that combination of quantum mechanics and pure disorder can lead to emergence of topological dimensions. Although d_{IR} is based on effective counting of which $p(d)$ has no a priori knowledge, $d_{\text{IR}} \geq d_{\text{max}}$ is an exact feature of the ensuing formalism. Possible connection of our results to recent findings of $d_{\text{IR}} \approx 2$ in Dirac near-zero modes of thermal quantum chromodynamics is emphasized.

Keywords: Anderson transition, localization, effective counting dimension, effective number theory, effective support, dimension content, emergent space

1. Introduction. Understanding spatial geometry of Anderson transitions [1] is an intriguing problem. Indeed, although studied quite extensively, the complicated structure of critical electronic states (see e.g. [2]) leaves room for new insights. Novel characterization may reveal unknown details of disorder-driven metal-insulator transitions and, for example, lead to deeper understanding of their renormalization group description [3].

Another reason to study the geometry of Anderson transitions arises by seeing them as quantum *dimension transitions*, a viewpoint taken in Ref. [4]. Using effective number theory (ENT) [5, 6], which entails a unique measure-based dimension d_{IR} [7, 8] for spaces with probabilities, it showed that the transition is a two-step dimension reduction

$$d_{\text{IR}} = 3 \longrightarrow \approx 8/3 \longrightarrow 0 \quad (1)$$

Here the flow is from extended to critical to localized state, and exponential localization was assumed. Remarkable property of the above is that these reductions are complete [9]. Indeed, probability doesn't leak away from subdimensional effective supports, and electron is fully confined to them in infinite volume. It is thus meaningful to say that the space available to quantum particle collapses into lower dimensional one under the influence of strong enough disorder. As such, it represents a mechanism for generating lower-dimensional spaces by simple combination of quantum mechanics and disorder.

While dimension is the most basic characteristic of space available to critical electron, this space may contain subsets with dimensions $d < d_{\text{IR}}$. Such substructure may be physically significant if electron mostly resides there. The aim of this work is to characterize the critical spatial geometry in such manner: we will compute the probability

distribution $p(d)$ that electron is present in space of dimension d . We refer to $p(d)$ as *dimension content* of Anderson criticality or that of probability distribution in general.

Critical states at Anderson transitions were recognized to have fractal-like features long ago, first interpreting them in analogy to scale-invariant fractals [10, 11] and later to more complex multifractals [12–15]. Formalism used in the latter mimics one that describes ultraviolet (UV) measure singularities occurring in turbulence and strange attractors (see e.g. [16, 17]). More recent works in the Anderson context are [18–22]. However, the focus of multifractal analysis doesn't make it convenient for computing $p(d)$. We thus proceed by proposing a method that organizes the calculation in terms of probabilities from the outset and zooms in on dimensions by degree of their actual presence. Moreover, d involved is simply the IR Minkowski dimension of a subset, and thus manifestly a measure-based dimension of space. In the ensuing multidimensionality formalism, wave function is

$$\begin{aligned} \text{subdimensional if} & \quad d_{\text{IR}} < D \\ \text{multidimensional if} & \quad p(d) \neq \delta(d - d_{\text{max}}) \\ \text{of proper dimension if} & \quad d_{\text{IR}} = d_{\text{max}} \end{aligned} \quad (2)$$

where $d_{\text{max}} = \sup \{d | p(d) > 0\}$, $D=3$ is the IR dimension of the underlying space, and $d_{\text{IR}} \geq d_{\text{max}}$ holds in general.

Before proceeding to define $p(d)$, we illustrate the idea on a “shovel” in $\mathbb{R}^{D=3}$ space (Fig. 1). The shovel consists of 2d square blade and 1d handle with uniformly distributed masses $M_b > 0$ and $M_h > 0$ respectively. If the relevance of space points is set by mass they carry, the probability of encountering the handle, the blade and the rest of space is $\mathcal{P} = M_h/(M_b+M_h)$, $1-\mathcal{P}$ and 0 respectively. Note that

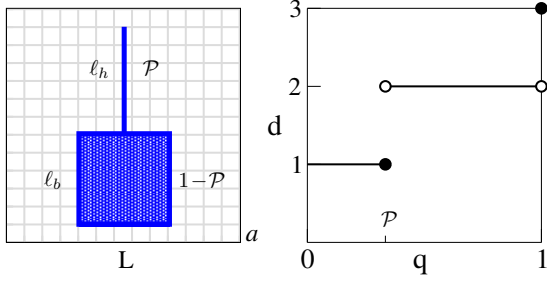


FIG. 1. The “shovel” (left) and $d(q)$ (right) associated with its UV dimension content in \mathbb{R}^3 . See discussion in the text.

UV cutoff a and IR cutoff L are also indicated.

Above we implicitly assumed that d is the usual UV dimension ($a \rightarrow 0$ at fixed L) in which case we have by inspection $p(d) = \mathcal{P} \delta(d-1) + (1-\mathcal{P}) \delta(d-2)$. But how would this $p(d)$ be concluded by a computer that cannot “see” and only processes regularized probability vectors $P(a) = (p_1, p_2, \dots, p_{N(a)})$? Here $N(a) = (L/a)^3$, p_i is the probability within elementary cube at point x_i of latticized space, and $a \in \{L/k \mid k = 2, 3, \dots\}$.

Anticipating that any number J of discrete dimensions $0 \leq d_1 < d_2 < \dots < d_J \leq 3$ with probabilities $\mathcal{P}_j > 0$ could be present, computer first orders p_i in each $P(a)$ so that $p_1 \geq p_2 \geq \dots \geq p_{N(a)}$. The rationale is that, with decreasing a , this increasingly better separates out populations related to different d_j . Indeed, the typical size of p associated with d_j is $\propto a^{d_j}$ and so $P(a)$ gradually organizes into J sequential blocks starting with d_1 . The above ordering in P will always be assumed from now on.

To detect possible blocks/dimensions, computer uses variable $q \in [0, 1]$ for cumulative probability, and associates with each $P(a)$ function $\nu(q, a)$, namely the number of first elements in $P(a)$ (space points) whose probabilities add to q . Keeping track of fractional boundary contributions at each q makes it a continuous, convex, increasing, piecewise linear function such that $\nu(0, a) = 0$ and $\nu(1, a) = N(a)$. Number of points in interval $(q - \epsilon, q]$ is $\nu(q, a) - \nu(q - \epsilon, a)$ and scales as $a^{-d(q, \epsilon)}$ for $a \rightarrow 0$. When processing $P(a)$ for the shovel, computer finds perfect scaling $(\ell_h/a) \times \epsilon/\mathcal{P}$ for $\epsilon \leq q \leq \mathcal{P}$, and $(\ell_b/a)^2 \times \epsilon/(1-\mathcal{P})$ for $\mathcal{P} + \epsilon < q < 1$. It will thus conclude $d(q)$ shown in Fig. 1 upon $\epsilon \rightarrow 0$. Value at $q=1$ represents the spatial complement of the shovel (zero probability). Collecting the probability of d , namely $p(d) = \int_0^1 dq \delta(d - d(q))$ produces the inspected result.

Two points are relevant here. (1) The above approach doesn’t change if continuous set of dimensions is present. In that case the obtained $d(q)$ is not piecewise constant, but rather a piecewise continuous non-decreasing function, possibly with constant parts identifying discrete dimensions. (2) IR case is fully analogous, but it is useful to recall the meaning of IR dimension ($L \rightarrow \infty$, a fixed) which is somewhat non-standard. Thus, if both ℓ_h and ℓ_b are fixed as $L \rightarrow \infty$ (usual case) then $p(d) = \delta(d)$ since populations at each q remain constant. However, if e.g. ℓ_b is fixed while handle responds by $\ell_h \propto L$ (shovel reaches

anywhere in space) then $p(d) = (1-\mathcal{P})\delta(d) + \mathcal{P}\delta(d-1)$.

2. The Formalism. We now define $p(d)$ in IR setting of Anderson transitions. Such analysis pertains to wave functions $\psi = \psi(r_i)$ on cubic lattice of $N(L) = (L/a)^D$ sites r_i , with L the IR regulator and a set to unity. With ψ we associate the probability vector $P = (p_1, p_2, \dots, p_{N=N(L)})$, where $p_i = \psi^\dagger \psi(r_i)$, the effective number of sites [5, 6]

$$\mathcal{N}_\star[\psi] = \sum_{i=1}^N \mathbf{n}_\star(Np_i) \quad , \quad \mathbf{n}_\star(c) = \min\{c, 1\} \quad (3)$$

and the cumulative count $\nu[q, \psi]$ defined as follows. Consider cumulative probabilities (q_0, q_1, \dots, q_N) with $q_0 = 0$ and $q_j = \sum_{i=1}^j p(i)$ for $j > 0$. Let $j(q)$, $q \in (0, 1)$ be the largest j such that $q_j < q$. Then $\nu[0, \psi] = 0$, $\nu[1, \psi] = N$ and

$$\nu[q, \psi] = j(q) + \frac{q - q_j}{q_{j+1} - q_j} \quad , \quad 0 < q < 1 \quad (4)$$

Recalling the order in P , $\nu[q, \psi]$ is increasing and convex.

Consider the Anderson model in orthogonal class [1]. With c_{r_i} the electron operators, the Hamiltonian is

$$\mathcal{H} = \sum_i \epsilon_{r_i} c_{r_i}^\dagger c_{r_i} + \sum_{i,j} c_{r_i}^\dagger c_{r_i - e_j} + h.c. \quad (5)$$

where e_j ($j=1, \dots, D$) are unit lattice vectors and random potentials $\epsilon_{r_i} \in [-W/2, +W/2]$ are uniformly distributed. Physics of the model involves averaging over disorder $\{\epsilon_{r_i}\}$. For \mathcal{N}_\star and ν of 1-particle eigenstates ψ at energy E we get

$$\mathcal{N}_\star[\psi] \rightarrow \mathcal{N}_\star(E, W, L) \quad , \quad \nu[q, \psi] \rightarrow \nu(q, E, W, L) \quad (6)$$

Keeping the dependence on E, W implicit, $L \rightarrow \infty$ behavior defines dimensional characteristics d_{IR} and $d(q)$ via

$$\mathcal{N}_\star(L) \propto L^{d_{\text{IR}}} \quad , \quad \nu(q, L) - \nu(q - \epsilon, L) \propto L^{d(q, \epsilon)} \quad (7)$$

with $d(q) = \lim_{\epsilon \rightarrow 0} d(q, \epsilon)$. Due to convexity of cumulative counts, $d(q, \epsilon)$ and $d(q)$ are non-decreasing. Probability density of finding IR dimension d in a state is then

$$p(d, \epsilon) = \int_0^1 dq \delta(d - d(q, \epsilon)) \quad , \quad p(d) = \lim_{\epsilon \rightarrow 0} p(d, \epsilon) \quad (8)$$

If $d(q)$ is differentiable at q , then $p(d = d(q)) = 1/d'(q)$. The range of $d(q)$, equal to support of $p(d)$, specifies IR dimensions occurring with non-zero probability in states of interest. It is a subset of $[d_{\min}, d_{\max}]$ where

$$d_{\min} = \inf\{d \mid p(d) > 0\} \quad , \quad d_{\max} = \sup\{d \mid p(d) > 0\} \quad (9)$$

Important feature in the ensuing formalism is that

$$d_{\max} \leq d_{\text{IR}} \leq D \quad (10)$$

Here the inequalities involving D are obvious and the last one can be most easily seen in discrete case. Indeed, let

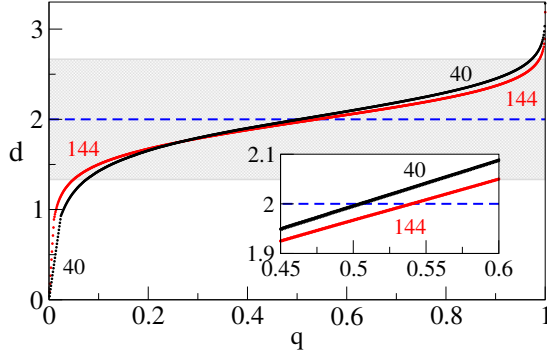


FIG. 2. Function $d(q, \epsilon, L)$ at $\epsilon = 10^{-3}$ for $L=40$ and $L=144$ (largest) systems. Shaded region marks the range $d \in [4/3, 8/3]$.

$p(d) = \sum_{j=1}^J \mathcal{P}_j \delta(d - d_j)$ with $0 \leq d_1 < \dots < d_J \leq D$, $\mathcal{P}_j > 0$, and assume that $d_{\text{IR}} < d_J = d_{\text{max}}$. Consider q such that $1 - \mathcal{P}_J < q < 1$. Then $\nu(q, L) - \nu(q - \epsilon, L) = \epsilon v(q, \epsilon, L) L^{d(q, \epsilon)}$ for sufficiently small ϵ , where $\lim_{\epsilon \rightarrow 0} d(q, \epsilon) = d_J$ and $\lim_{\epsilon \rightarrow 0} \lim_{L \rightarrow \infty} v(q, \epsilon, L) = v(q) > 0$. The size of individual $p = \epsilon / (\nu(q, L) - \nu(q - \epsilon, L))$ in this population is then $L^{-d(q, \epsilon)} / v(q, L, \epsilon)$. Hence, if $d_J < D$ then $\min\{1, Np\}$ in definition of N_* yields 1 for sufficient L and ϵ , while if $d_J = D$ it yields $1/v(q)$. In both cases, the contribution of this population to N_* is $\propto L^{d_J}$. Hence, $d_{\text{IR}} \geq d_J$ which contradicts the assumption and leads to (10).

3. Anderson Criticality. We now perform the dimensional analysis for critical states of $D=3$ Anderson Hamiltonian (3) with periodic boundary conditions at critical point $(E_c, W_c) = (0, 16.543(2))$ [23]. Calculation in Ref. [4] yielded $d_{\text{IR}} = 2.665(2) \approx 8/3$. For $d(q)$ we follow [4], keeping track of dimension defined at finite L and extrapolating it directly. In particular,

$$d(q, \epsilon, L) = \frac{1}{\log s} \log \frac{\nu(q, L) - \nu(q - \epsilon, L)}{\nu(q, L/s) - \nu(q - \epsilon, L/s)} \quad (11)$$

with fixed $s > 1$, and $d(q, \epsilon) = \lim_{L \rightarrow \infty} d(q, \epsilon, L)$. In the analysis we set $s = 2$. For 34 sizes in the range $16 \leq L \leq 144$, two near-zero eigenmodes were computed at 40k–100k disorder samples using the JADAMILU package [24]. We set $\epsilon = 10^{-3}$, thus splitting the interval $q \in [0, 1]$ into 1000 bins and evaluating $d(q_b, \epsilon, L)$ at $q_b = b \times 10^{-3}$, $b = 1, \dots, 1000$. We verified that this is fine enough to directly represent $\epsilon \rightarrow 0$ limits for our purposes.

Given that, we show $d(q, L)$ at $L = 40$ and $L = 144$ in Fig. 2. Important feature of the obtained behavior is the flatness in the middle part of q , indicating large probabilities for dimensions in the corresponding range. Increase of L results in flatter $d(q, L)$ and yet sharper range of prominent dimensions. Visible linear parts at small q mark regions where finite-size effects yield $\nu(q)$ non-convex. Their extent shrinks toward zero with growing L . Linearity was imposed to keep the behavior regular.

The corresponding $p(d, L)$ obtained via (8) are shown in Fig. 3. We observe sharp peaks of decreasing width, centered at $d_m \approx 2$. The error bars, too small to be visible,

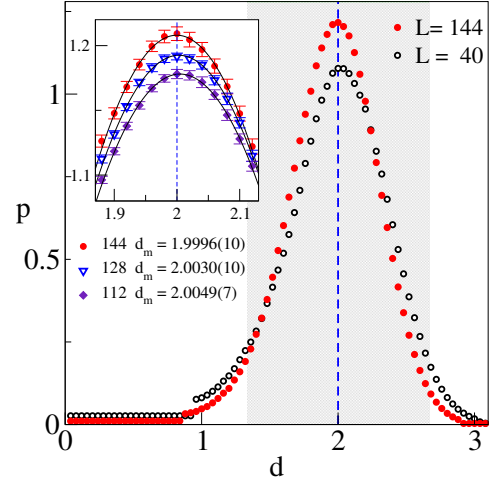


FIG. 3. Function $p(d, \epsilon, L)$ at $\epsilon = 10^{-3}$ for $L=40$ and $L=144$ (largest) systems. Shaded region marks the range $d \in [4/3, 8/3]$.

were obtained via Jackknife procedure with respect to disorder samples. Stability of d_m and its proximity to 2 is quite remarkable as shown in the inset for the largest sizes studied. Quoted values were obtained from quadratic fits in the displayed vicinity of the maximum. The constant parts at small d correspond to linear segments in Fig. 2.

Among key characteristics of dimension content $p(d)$ is its support, i.e. dimensions that can contribute to physical processes with non-zero probability density. The above properties of $p(d, L)$ imply that the support in fact spans $[d_{\text{min}}, d_{\text{max}}]$, and its specification thus reduces to finding d_{min} and d_{max} . To that effect, we evaluate probabilities $p(d < d_0, L)$ of dimensions smaller than d_0 , and vary d_0 upward. For each d_0 , $p(d < d_0, L)$ is $L \rightarrow \infty$ extrapolated by fitting to a constant with general power correction. The result, shown in Fig. 4 panel (a), features a probability threshold turning on near $d_0 = 1.3$. We take $d_0 = 4/3$ as a reference value: in panel (c) we show its extrapolation leading to a clean statistical zero. Analogous procedure based on $p(d > d_0)$ yields results shown in panels (b), (d) with $d_0 = 8/3$ referencing the other threshold.

Given the strong dominance of d_m , the second key question is whether d_m could be a discrete dimension in Anderson critical states. This would mean that, in $L \rightarrow \infty$ limit, $d(q, L)$ (see Fig. 2) develops a strictly constant part in certain range of q . We will test this possibility for the observed $d_m = 2$ via the following procedure. Given a $d(q, L)$, we find $q_2(L)$ such that $d(q_2, L) = 2$ and calculate

$$I(\rho, L) = \int_{q_2 - \rho/2}^{q_2 + \rho/2} dq \left(2 - d(q, L) \right)^2 \quad (12)$$

which is only zero if $d(q, L) = 2$ on the interval. For given ρ , we perform $L \rightarrow \infty$ extrapolation via fit to a constant $I(\rho)$ with general power correction. Fitting data for systems with $L > 28$ leads to results shown in Fig. 5 (circles). Notice a steep decay of $I(\rho)$ with decreasing ρ , reaching

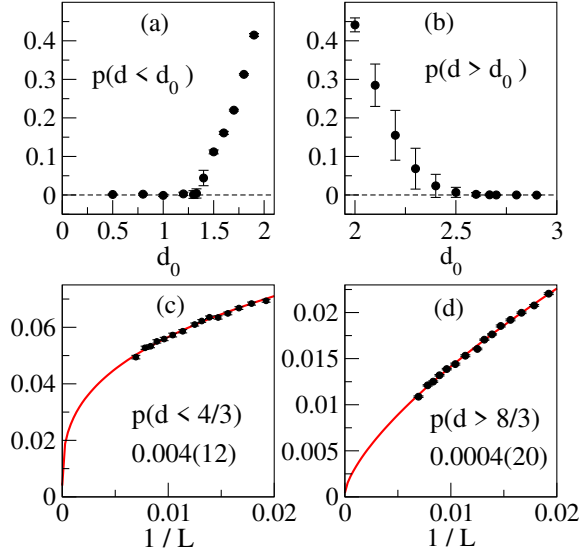


FIG. 4. Probabilities $p(d < d_0)$ and $p(d > d_0)$ in $L \rightarrow \infty$ limit. Panels (c), (d) show extrapolations for $d_0 = 4/3$ and $d_0 = 8/3$.

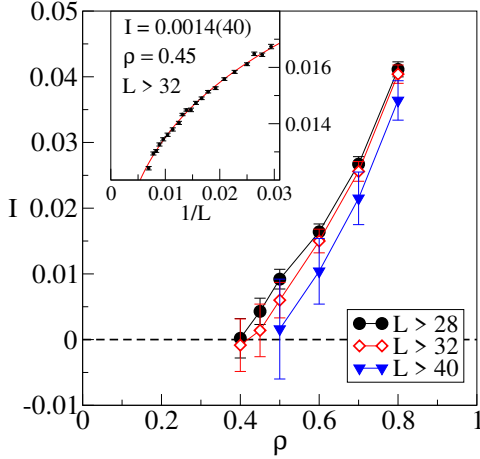


FIG. 5. Function $I(\rho, L \rightarrow \infty)$ obtained by fitting in L -ranges containing increasingly larger lattices. Inset shows example of a fit in the vicinity of ρ_0 such that $I(\rho_0) \approx 0$.

$I \approx 0$ at $\rho \approx 0.4$ with errors becoming large below this point. While this could simply indicate a very steep analytic behavior of $I(\rho)$, further analysis suggests otherwise. Indeed, restricting fits to larger systems, namely $L > 32$ (diamonds) and $L > 40$ (triangles), results in increasingly steeper decay toward zero at yet larger ρ . Natural interpretation of these tendencies is that $I(\rho) \equiv 0$ for $\rho < \rho_0 \approx 0.5$, pointing to discrete nature of d_m .

The synthesis of our results suggests the following form of spatial dimension content at Anderson criticality

$$p(d) = \mathcal{P} \delta(d - d_m) + (1 - \mathcal{P}) \pi(d) \quad (13)$$

where $\pi(d)$ is a continuous probability distribution with support on interval $[d_{\min}, d_{\max}]$. The parameters are

$$d_m \approx 2, \quad d_{\min} \approx 4/3, \quad d_{\max} \approx 8/3, \quad \mathcal{P} \gtrsim 1/2 \quad (14)$$

where we estimate the accuracy of d_m at couple % and that of d_{\min} , d_{\max} at couple %. Graphical representation of this result in terms of $d(q)$ and $p(d)$ is shown in Fig. 6.

4. Discussion. We proposed to characterize probability distributions on metric spaces by their measure-based effective dimension (d_{UV} or d_{IR}) [5–8] and the associated *dimension content* $p(d)$. The method was applied to the structure of critical states in $D=3$ Anderson transition (O class). Here $p(d)$ identifies dimensions of regions where electron can in fact be found, i.e. those relevant to its physics. Critical wave functions are subdimensional, multidimensional and our new results are summarized by Eqs. (13) and (14). Few comments should be made.

(i) The picture of Anderson transition as spatial dimension transformation (1) receives key refinements by virtue of $p(d)$. Indeed, although critical electron is fully confined to spatial effective support \mathcal{S}_* of Minkowski dimension $d_{IR} \approx 8/3$ [4, 9], its key substructure has $d_m \approx 2$, and the continuum of lower and higher-dimensional features is also present. Geometrically, \mathcal{S}_* may thus also be viewed as surface-like structure endowed with complex lower-dimensional “hair” and higher-dimensional “halo”.

(ii) Our results suggest that d_m is a discrete dimension and that it may assume an exactly topological value $d_m = 2$. [Mathematical meaning of “topological” in the context of IR dimension would of course need some clarification.] This invokes a possibility that quantum mechanics combined with pure disorder can lead to emergence of integer dimensions. Apart from understanding of Anderson transitions, variations on such dynamics could find relevance in modeling emergent space in early universe. More detailed description of this geometry would be needed.

(iii) Connection between d_{IR} and $p(d)$ results from built-in additivity which makes them measure-based: in case of d_{IR} it is additivity of effective counting with respect to combining the systems [5, 6], and for $d(q)$ the familiar additivity of ordinary counting. This aspect is key to interpretation of these concepts as spatial dimensions. Indeed, it is because Hausdorff measure and Minkowski count properly quantify volume that dimensions based on them became useful and accepted characteristics of space.

(iv) It is natural to ask whether some features of the described spatial structure have analogues in the multi-

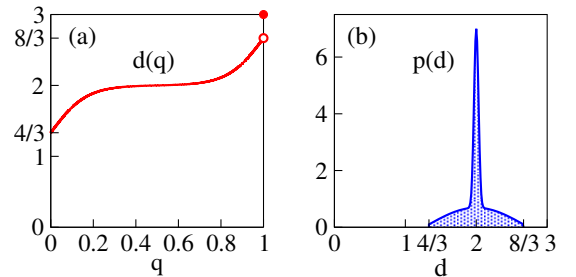


FIG. 6. Graphical representation of concluded dimensional content at criticality. Narrow spike in (b) represents δ -function.

fractal approach [16, 17] adopted to IR Anderson setting via moment method [25]. Here the focus is on the so called dimensional spectrum $f(\alpha)$. Inner workings of the method give special status to information dimension [26] in a way somewhat similar to d_m . It would be interesting to study the possible association between the two in detail. (See also debate regarding d_{IR} in Refs. [27, 28].)

(v) Our data is consistent with critical wave functions being of proper dimension ($d_{\text{IR}} = d_{\text{max}}$). However, albeit state of the art, their statistical power is not sufficient to reach sharper conclusion at this point.

(vi) Our findings acquire another angle in light of recent results [7, 29] in quantum chromodynamics (QCD). The original proposal that Anderson-like mobility edge $\lambda_A > 0$ appears in QCD Dirac spectrum upon thermal chiral transition [30, 31], worked out by Refs. [32–34], became more structured. Indeed, existence of a new mobility edge $\lambda_{\text{IR}} \equiv 0$ has been concluded and its simultaneous appearance with λ_A at temperature T_{IR} was conjectured [29]. Here T_{IR} marks the transition to phase featuring IR scale invariance of glue fields [35]. Approach to IR criticality ($\lambda \rightarrow \lambda_{\text{IR}}^+$) was found to proceed via $d_{\text{IR}} \approx 2$ Dirac modes [7], with topological origin of the dimension suspected. Clarifying a possible relation of this to $d_m \approx 2$ found here may shed new light on QCD–Anderson localization connection.

(vii) The proposed IR/UV guises of multidimensionality formalism easily extend to more general situations without metric. Here the sequence $\{O_k\}$ involving collections $O_k = (o_{k,1}, o_{k,2}, \dots, o_{k,N_k})$ with increasing number N_k of arbitrary objects comes with associated sequence $\{P_k\}$ of relevance (probability) vectors. The role of $d_{\text{IR}}/d_{\text{UV}}$ is taken by the effective counting dimension $0 \leq \Delta \leq 1$ defined via scaling $N_*[P_k] \propto N_k^\Delta$ for $k \rightarrow \infty$ [8]. Dimension function $d(q)$ is replaced by analogous $\gamma(q)$ and dimension content $p(d)$ by $p(\gamma)$. The target ($k \rightarrow \infty$) effective collection defined by $\{O_k\}, \{P_k\}$ is then

$$\begin{aligned} &\text{subdimensional if} && \Delta < 1 \\ &\text{multidimensional if} && p(\gamma) \neq \delta(\gamma - \gamma_{\text{max}}) \\ &\text{of proper dimension if} && \Delta = \gamma_{\text{max}} \end{aligned} \quad (15)$$

where $\gamma_{\text{max}} = \sup \{\gamma | p(\gamma) > 0\}$ and $\gamma_{\text{max}} \leq \Delta$.

P.M. was supported by Slovak Grant Agency VEGA, Project n. 1/0101/20.

* ihorv2@g.uky.edu

† peter.markos@fmph.uniba.sk

- [1] P. W. Anderson, *Phys. Rev.* **109**, 1492 (1958).
- [2] O. Schenk, M. Bollhöfer, and R. A. Römer, *SIAM Review* **50**, 91 (2008).
- [3] E. Abrahams, P. W. Anderson, D. C. Licciardello, and T. V. Ramakrishnan, *Phys. Rev. Lett.* **42**, 673 (1979).
- [4] I. Horváth and P. Markoš, *Phys. Rev. Lett.* **129**, 106601 (2022), [arXiv:2110.11266](https://arxiv.org/abs/2110.11266) [cond-mat.dis-nn].
- [5] I. Horváth and R. Mendris, *Entropy* **22**, 1273 (2020), [arXiv:1807.03995](https://arxiv.org/abs/1807.03995) [quant-ph].
- [6] I. Horváth, *Quantum Rep.* **3**, 534 (2021), [arXiv:1809.07249](https://arxiv.org/abs/1809.07249) [quant-ph].
- [7] A. Alexandru and I. Horváth, *Phys. Rev. Lett.* **127**, 052303 (2021), [arXiv:2103.05607](https://arxiv.org/abs/2103.05607) [hep-lat].
- [8] I. Horváth, P. Markoš, and R. Mendris, (2022), [arXiv:2205.11520](https://arxiv.org/abs/2205.11520) [hep-lat].
- [9] I. Horváth and P. Markoš, (2022), [arXiv:2207.13569](https://arxiv.org/abs/2207.13569) [cond-mat.dis-nn].
- [10] H. Aoki, *Journal of Physics C: Solid State Physics* **16**, L205 (1983).
- [11] C. M. Soukoulis and E. N. Economou, *Phys. Rev. Lett.* **52**, 565 (1984).
- [12] C. Castellani and L. Peliti, *Journal of Physics A: Mathematical and General* **19**, L429 (1986).
- [13] S. N. Evangelou, *Journal of Physics A: Mathematical and General* **23**, L317 (1990).
- [14] M. Schreiber and H. Grussbach, *Phys. Rev. Lett.* **67**, 607 (1991).
- [15] M. Janssen, *Int. J. Mod. Phys. B* **8**, 943 (1994).
- [16] K. Falconer, *Fractal Geometry: Mathematical Foundations and Applications*, 3rd ed. (Wiley, 2014).
- [17] T. C. Halsey, M. H. Jensen, L. P. Kadanoff, I. Procaccia, and B. I. Shraiman, *Phys. Rev. A* **33**, 1141 (1986).
- [18] A. Mildenberger, F. Evers, and A. D. Mirlin, *Physical Review B* **66**, 033109 (2002).
- [19] L. J. Vasquez, A. Rodriguez, and R. A. Römer, *Physical Review B* **78**, 195106 (2008).
- [20] A. Rodriguez, L. J. Vasquez, and R. A. Römer, *Physical Review B* **78**, 195107 (2008).
- [21] A. Rodriguez, L. J. Vasquez, K. Slevin, and R. A. Römer, *Physical Review B* **84** (2011), [10.1103/physrevb.84.134209](https://arxiv.org/abs/10.1103/physrevb.84.134209).
- [22] L. Ujfalusi and I. Varga, *Phys. Rev. B* **91**, 184206 (2015).
- [23] K. Slevin and T. Ohtsuki, *Journal of the Physical Society of Japan* **87**, 094703 (2018).
- [24] M. Bollhöfer and Y. Notay, *Comp. Phys. Comm.* **177**, 951 (2007).
- [25] F. Evers and A. D. Mirlin, *Reviews of Modern Physics* **80**, 1355 (2008).
- [26] P. Grassberger, *Physics Letters A* **107**, 101 (1985).
- [27] I. S. Burmistrov, *arXiv e-prints* (2022), [arXiv:2210.10539](https://arxiv.org/abs/2210.10539) [cond-mat.dis-nn].
- [28] I. Horváth and P. Markoš, *arXiv e-prints* (2022), [arXiv:2212.02912](https://arxiv.org/abs/2212.02912) [cond-mat.dis-nn].
- [29] A. Alexandru and I. Horváth, *Phys. Lett. B* **833**, 137370 (2022), [arXiv:2110.04833](https://arxiv.org/abs/2110.04833) [hep-lat].
- [30] A. M. Garcia-Garcia and J. C. Osborn, *Nucl. Phys. A* **770**, 141 (2006), [arXiv:hep-lat/0512025](https://arxiv.org/abs/hep-lat/0512025).
- [31] A. M. Garcia-Garcia and J. C. Osborn, *Phys. Rev. D* **75**, 034503 (2007), [arXiv:hep-lat/0611019](https://arxiv.org/abs/hep-lat/0611019).
- [32] T. G. Kovacs and F. Pittler, *Phys. Rev. Lett.* **105**, 192001 (2010), [arXiv:1006.1205](https://arxiv.org/abs/1006.1205) [hep-lat].
- [33] M. Giordano, T. G. Kovacs, and F. Pittler, *Phys. Rev. Lett.* **112**, 102002 (2014), [arXiv:1312.1179](https://arxiv.org/abs/1312.1179) [hep-lat].
- [34] L. Ujfalusi, M. Giordano, F. Pittler, T. G. Kovács, and I. Varga, *Phys. Rev. D* **92**, 094513 (2015), [arXiv:1507.02162](https://arxiv.org/abs/1507.02162) [cond-mat.dis-nn].
- [35] A. Alexandru and I. Horváth, *Phys. Rev. D* **100**, 094507 (2019), [arXiv:1906.08047](https://arxiv.org/abs/1906.08047) [hep-lat].